Supporting Information File:

Nanopore Detection of 8-Oxo-7,8-dihydro-2'-deoxyguanosine in Immobilized Single-stranded DNA via Adduct Formation to the DNA Damage Site

Anna E. P. Schibel, Na An, Qian Jin, Aaron M. Fleming, Cynthia J. Burrows*, and Henry S. White*

Department of Chemistry, University of Utah, 315 S. 1400 East, Salt Lake City, UT 84112-0850

Complete Reference 10

Branton, D.; Deamer, D. W.; Marziali, A.; Bayley, H.; Benner, S. A.; Butler, T.; Di Ventra, M.; Garaj, S.; Hibbs, A.; Huang, X.; Jovanovich, S. B.; Krstic, P. S.; Lindsay, S.; Ling, X. S.; Mastrangelo, C. H.; Meller, A.; Oliver, J. S.; Pershin, Y. V.; Ramsey, J. M.; Riehn, R.; Soni, G. V.; Tabard-Cossa, V.; Wanunu, M.; Wiggin, M.; Schloss, J. A. *Nat. Biotech.* **2008**, *26*, 1146-1153.

Experimental Procedures

Reagents for Adduct Synthesis. Gly-Pro-Arg-Pro amide, spermine, spermidine, benzylamine, D-(+)-glucosamine, N^{α}-acetyllysine methyl ester hydrochloride, and Na_2IrCl_6, were purchased from commercial suppliers and used without further purification.

DNA preparation and purification procedures. The 3'-biotinylated oligodeoxynucleotides (ODN) were synthesized from commercially available phosphoramidites (Glen Research, Sterling, VA) by the DNA-Peptide Core Facility at the University of Utah. After synthesis, each ODN was cleaved from the synthetic column and deprotected according to the manufacturer's protocols,

followed by purification using a semi-preparation ion-exchange HPLC column with a linear gradient of 25% to 100% B over 30 min while monitoring absorbance at 260 nm (A = 20 mM Tris, 1 M NaCl pH 7 in 10% CH_3CN/90% ddH_2O, B = 10% CH_3CN/90% ddH_2O, flow rate = 3 mL/min). The identities and purities of the ODNs were determined by negative ion electron spray (ESI^-) on a Micromass Quattro II mass spectrometer equipped with Zspray API source in the mass spectrometry laboratory at the Department of Chemistry, University of Utah.

Synthesis of ODN-hydantoin/ODN-Sp-NR products. The ODN-hydantoin/ODN-Sp-NR products were synthesized using the methodology previously established by the Burrows laboratory.[1,2,3] Briefly, the **ODN-Gh** products were produced by incubating OG-containing oligomers (10 μM, 1 nmole) in ddH_2O at 4 ^oC for 30 min; 12 equivalents of Na_2IrCl_6 (120 μM, 12 nmoles) were titrated into the ODN samples. After a 30 min incubation, the reactions were terminated with Na_2EDTA (pH 8, 1 mM, 100 nmoles). The **ODN-Sp** products were synthesized by allowing the OG-containing oligomers (10 μM, 1 nmole) in 75 mM NaP_i buffer (pH 7.4) to incubate at 45 ^oC for 30 min, followed by addition of 12 equivalents of Na_2IrCl_6 (120 μM, 12 nmoles), and Na_2EDTA (pH 8, 1 mM, 100 nmoles) was used to quench the oxidant after the reactions proceeded for 30 min.

The syntheses of **ODN-Sp-NRs** were achieved by thermally equilibrating the OG-containing oligomers (10 μM, 1 nmole) and various amines (2 mM, 200 nmoles) in 75 mM NaPi buffer (pH 8.0) at 45 ^oC for 30 min; then 15 equivalents of Na_2IrCl_6 (150 μM, 15 nmoles) were titrated into the samples that were then left for 30 min. The reactions were quenched the same way as previously described.

All the products were purified by an analytical ion-exchange HPLC column with a linear gradient of 25% to 100% B over 30 min while monitoring absorbance at 260 nm (A = 20 mM Tris, 1 M NaCl pH 7 in 10% CH_3CN/90% ddH_2O, B = 10% CH_3CN/90% ddH_2O, flow rate = 1

mL/min); see Table SI 1. *ODN-Sp-spermine and ODN-Sp-spermidine products were used immediately due to their instability.* [2]

Chemicals and Materials. Aqueous solutions mentioned below were prepared using >18 MΩ·cm ultrapure water from a Barnstead E-pure water purifier. KCl (Sigma-Aldrich), trizma base (Sigma-Aldrich), EDTA (Mallinckrodt Chemicals), and HCl (EMD) were used as received. A buffered electrolyte solution of 1.0 M KCl, 25 mM Tris-HCl, and 1.0 mM EDTA (pH 7.9) was prepared and used for all ion channel recording measurements. The buffered electrolyte solution was filtered using a sterile 0.22 mm Millipore vacuum filter (Fisher Scientific). The wild type protein channel α-hemolysin (αHL), isolated from *Staphylococcus aureus* as a monomer, was obtained as a lyophilized powder from List Biological Laboratories and stored at concentration of 0.5 mg αHL per mL ultra pure water in a -20 °C freezer. Upon use, the αHL solution was diluted to a concentration of 0.05 mg αHL per mL using the above mentioned buffered electrolyte and added directly to the experimental cell. The phospholipid 1,2-diphytanoyl-*sn*-glycero-3-phosphocholine (DPhPC) was purchased from Avanti Polar Lipids as a powder and stored in a -20 °C freezer. Upon use, the DPhPC powder was dispersed in decane (Fisher Scientific) to a concentration of 10 mg DPhPC per mL decane. Glass nanopore membranes (GNMs) were fabricated as previously described,[4,5] and before use as a bilayer support, were silanized in 2% (v:v) 3-cyanopropyldimethylchlorosilane in acetonitrile (Fisher Scientific) overnight.[6] Ag/AgCl electrodes were prepared by soaking silver wire (0.25 mm diameter, Alfa Aesar) in bleach. All DNA oligomers studied were obtained as described above, and DNA molecule binding to streptavidin was achieved by mixing DNA and streptavidin at a 4:1 ratio and incubating at room temperature for 10 minutes.

Immobilization Ion Channel Recording Measurements. Current-time (*i-t*) measurements were performed using a custom built high-impedance, low noise amplifier and data acquisition system (Electronic Bio Sciences, San Diego CA. Before use, a GNM was rinsed with ethanol and ultra

pure water, and finally filled with buffered electrolyte. The GNM was positioned within the EBS DC System via a pipette holder (Dagan Corporation), where the back end was sealed to a pressure gauge and 10 mL gas-tight syringe (Hamilton). An Ag/AgCl electrode wire was positioned inside the GNM and a second Ag/AgCl electrode was positioned in the experimental cell, external to the GNM. The same buffered electrolyte used to fill the GNM was added to the EBS DC System experimental cell, αHL was also added to the experimental cell (external to the GNM). Voltage was applied across the GNM orifice, *cis* vs. *trans* with respect to the αHL channel, and external vs. internal with respect to the GNM, and the resultant current was measured as a function of time.

Suspended bilayers were generated through painting. To form a suspended bilayer, a plastic pipette tip (gel-loading tips, flat, 1-200 μL, 0.4 mm) was filled with lipid solution and gently pulled across the GNM face, over the orifice. The establishment of a bilayer was confirmed by observing a drop in conductance as voltage was applied across the GNM orifice; an open pore has a resistance of approximately 10 MΩ, while a bilayer suspended across a GNM exhibits a resistance of around 100 GΩ.[6] After bilayer formation, a pressure was applied to the back of the GNM for protein channel reconstitution to occur.[6] Strep-Btn DNA was added to the cell in 100-200 nM increments. DNA was captured and held using an applied voltage of -120 mV (*cis* vs. *trans*), and released by reversing the bias. The modified sample of interest was added to the experimental cell first, and after an adequate number of blockage events are collected, a second control sample, Strep-Btn C_{40}, was added to the cell to provide a reference position. Data were collected with a 10 kHz low pass filter, and 50 kHz data acquisition rate.

DNA Immobilization Data Analysis. Only capture events longer than 1 second were included in data analysis. All event current blockage values (I) were normalized by the immediately preceding open channel current (I_o), and expressed as $\%I/I_o$. The Strep-Btn C_{40} $\%I/I_o$ peak position was set as the reference position 0. $\%I/I_o$ for all other molecules is reported relative to

Strep-Btn C_{40}; more blocking $\%I/I_o$ values are negative relative to Strep-Btn C_{40} and less blocking $\%I/I_o$ values are positive relative to Strep-Btn C_{40}.

Table SI 1. Characterization of the oligonucleotides.

Name	HPLC retention time (min)	Mass	
		Expected	Observed
C_{40}	14.5	12075.2	12075.3
$C_{39}G_{\omega 14}$	14.4	12115.3	12116.7
$C_{39}T_{\omega 14}$	14.4	12090.3	12089.6
$C_{39}A_{\omega 14}$	14.4	12099.3	12099.2
$C_{39}OG_{\omega 14}$	13.9	12131.3	12131.2
$C_{39}Sp_{\omega 14}$	14.2/14.5	12147.3	12163.2[a]
$C_{39}Gh_{\omega 14}$	13.7	12121.3	12137.5[a]
$C_{39}Bz_{\omega 14}$	13.4	12236.4	12236.8
$C_{39}GlcN_{\omega 14}$	12.7	12308.5	12308.8
$C_{39}Spd_{\omega 14}$	12.9	12274.6	12276.8
$C_{39}Spm_{\omega 14}$	12.8	12331.7	NA
$C_{39}Lys_{\omega 14}$	13.9/14.1	12331.4	12348.0[a]
$C_{39}GPRP_{\omega 14}$	11.3/11.9	12553.8	12553.6
$KrasG_{\omega 14}$	12.0	12864.1	12864.8
$KrasOG_{\omega 14}$	12.0	12880.1	12880.0
$KrasSp_{\omega 14}$	12.1/12.2	12896.1	12895.2
$KrasGh_{\omega 14}$	11.5/11.7	12870.1	12885.9[a]
$KrasSpm_{\omega 14}$	10.8	13030.4	NA

NA: not available due to instability of the adduct.
a: Products showed oxidation of the biotin during synthesis.

Figure SI 1. Example *i-t* trace and %I/I_o histogram for Strep-Btn C_{40}. Strep-Btn C_{40} current blockages result in a single, sharp, prominent %I/I_o peak. Strep-Btn C_{40} consistently yielded a single, sharp %I/I_o peak, and since all modifications discussed below are present within a C_{40} background, Strep-Btn C_{40} was used as a reference molecule. %I/I_o histograms in the text and in the following figures for single-modified base substitutions are plotted relative to %I/I_o for Strep-Btn C_{40} peak position, which is assigned a value of 0.

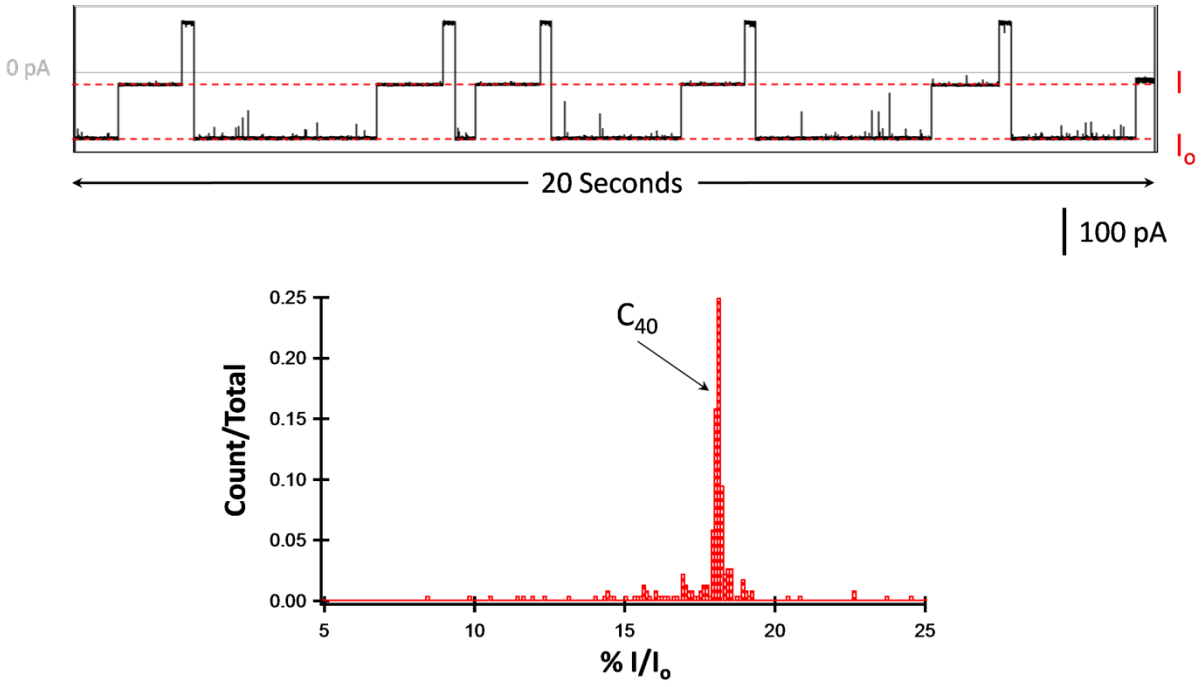

Figure SI 2. Example *i-t* trace for Strep-Btn $C_{39}G_{\omega 14}$ and $\%I/I_o$ histogram compared with Strep-Btn C_{40}.

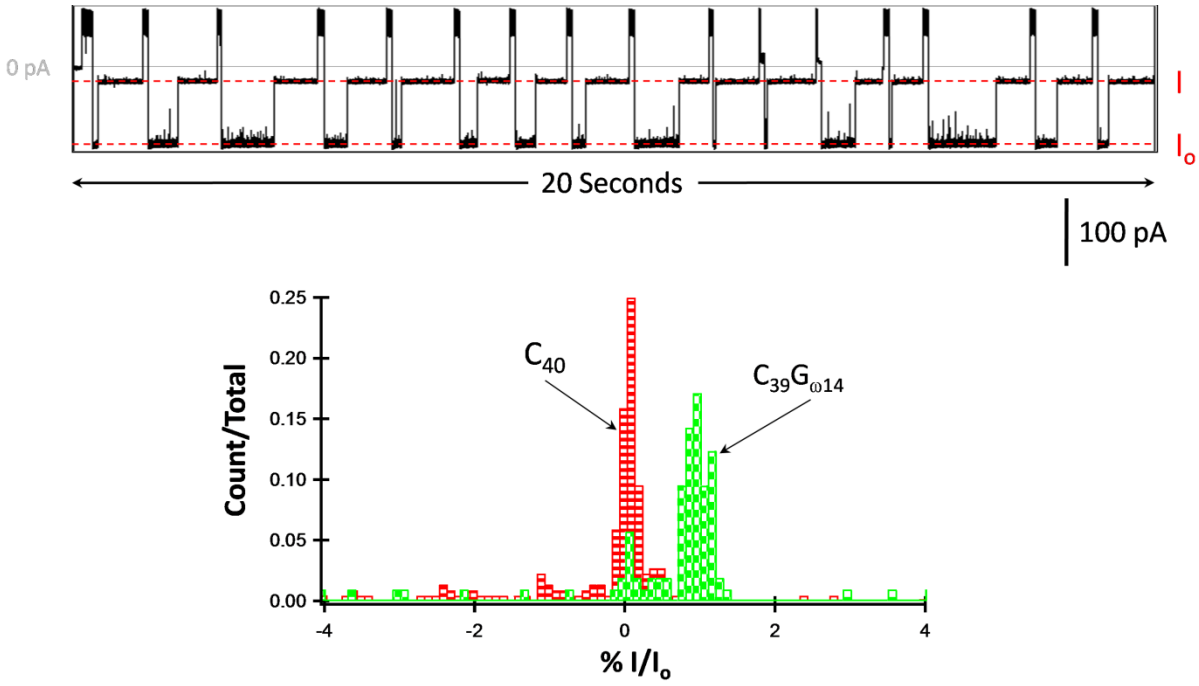

.

Figure SI 3. Example *i-t* trace for Strep-Btn $C_{39}OG_{\omega 14}$ and $\%I/I_o$ histogram compared with Strep-Btn C_{40}.

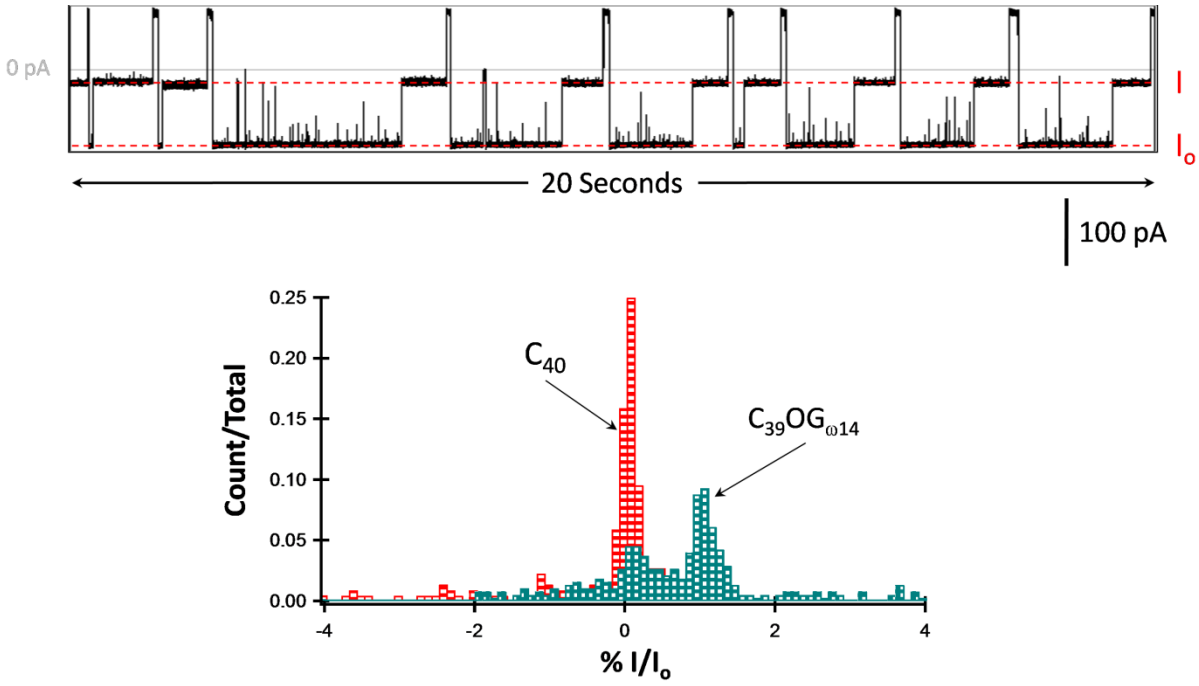

Figure SI 4. Example *i-t* traces for Strep-Btn $C_{39}Sp_{\omega 14}$ (upper) and Strep-Btn $C_{39}Gh_{\omega 14}$ (lower), and their respective $\%I/I_o$ histograms compared with Strep-Btn C_{40}.

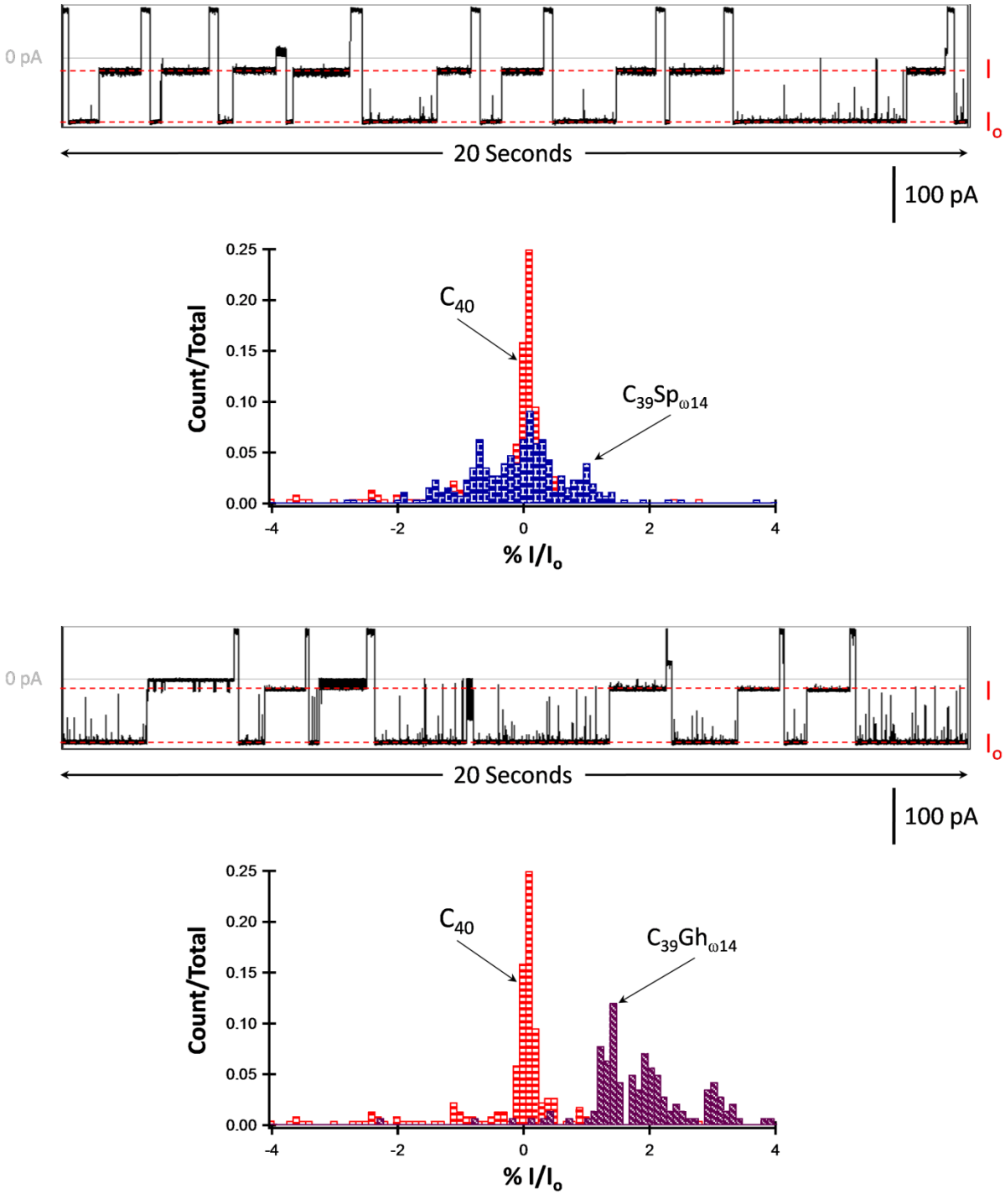

Figure SI 5. Example *i-t* trace for Strep-Btn $C_{39}Lys_{\omega 14}$ and the resulting $\%I/I_o$ histogram compared with Strep-Btn C_{40}. The lysine adduct produced multiple current blockage levels and noise amplitudes.

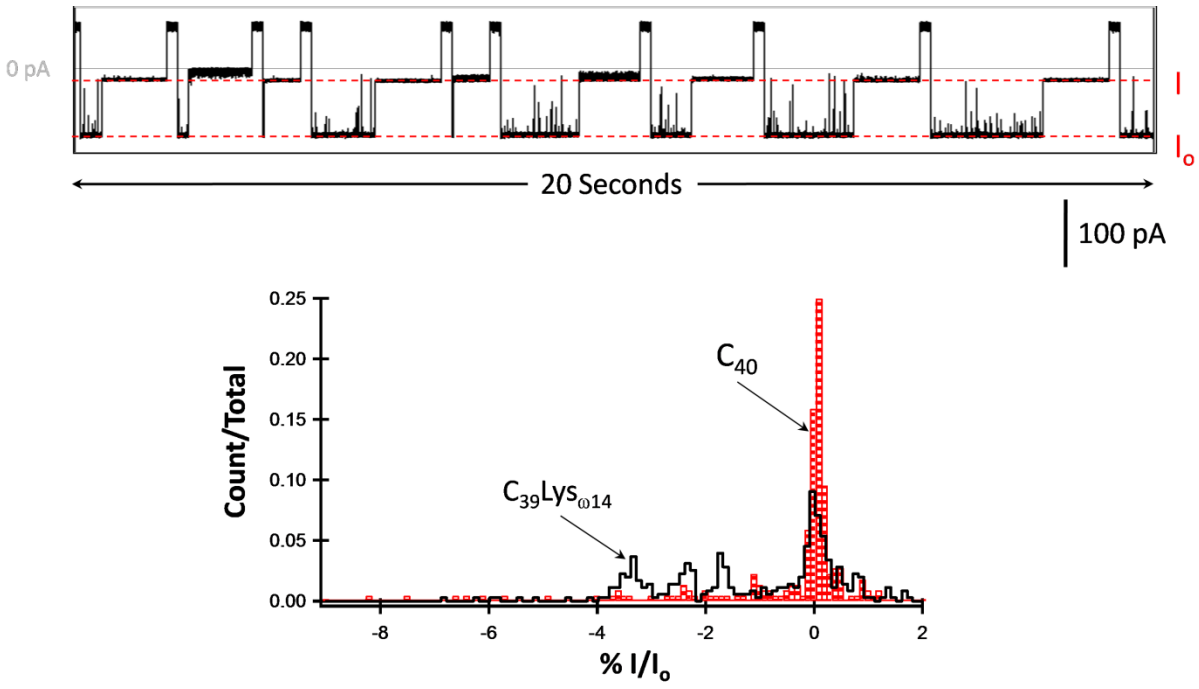

Figure SI 6. Example *i-t* traces for Strep-Btn $C_{39}Bz_{\omega 14}$ (upper) and Strep-Btn $C_{39}GlcN_{\omega 14}$ (lower) and the resulting $\%I/I_o$ histograms compared with Strep-Btn C_{40}. Both adducts produced multiple current blockage levels and noise amplitudes. Although the glucosamine adduct is a six-membered ring similar to the benzylamine adduct, it contains hydroxyl groups and is not aromatic.

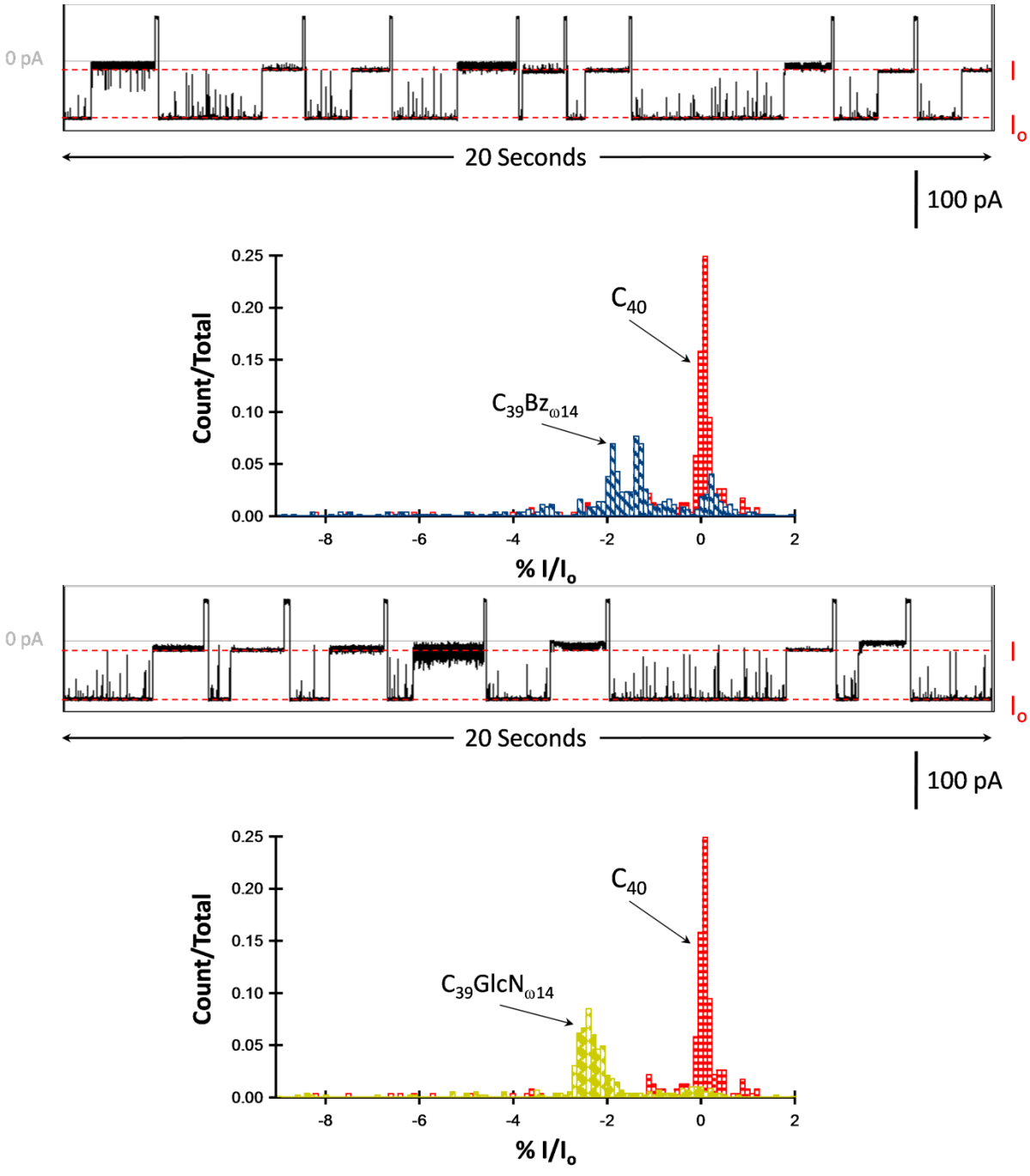

Figure SI 7. Example *i-t* traces for Strep-Btn $C_{39}Spd_{\omega 14}$ (upper) and Strep-Btn $C_{39}Spm_{\omega 14}$ (lower) and the resulting $\%I/I_o$ histograms compared with Strep-Btn C_{40}. Both adducts are linear and contain amine groups, with spermine being the longer of the two. $\%I/I_o$ histograms for both show multiple peak levels, but similar levels of noise. Both displayed less variable current blockage and noise levels relative to the cyclic adducts (Trp, Bz, and GlcN).

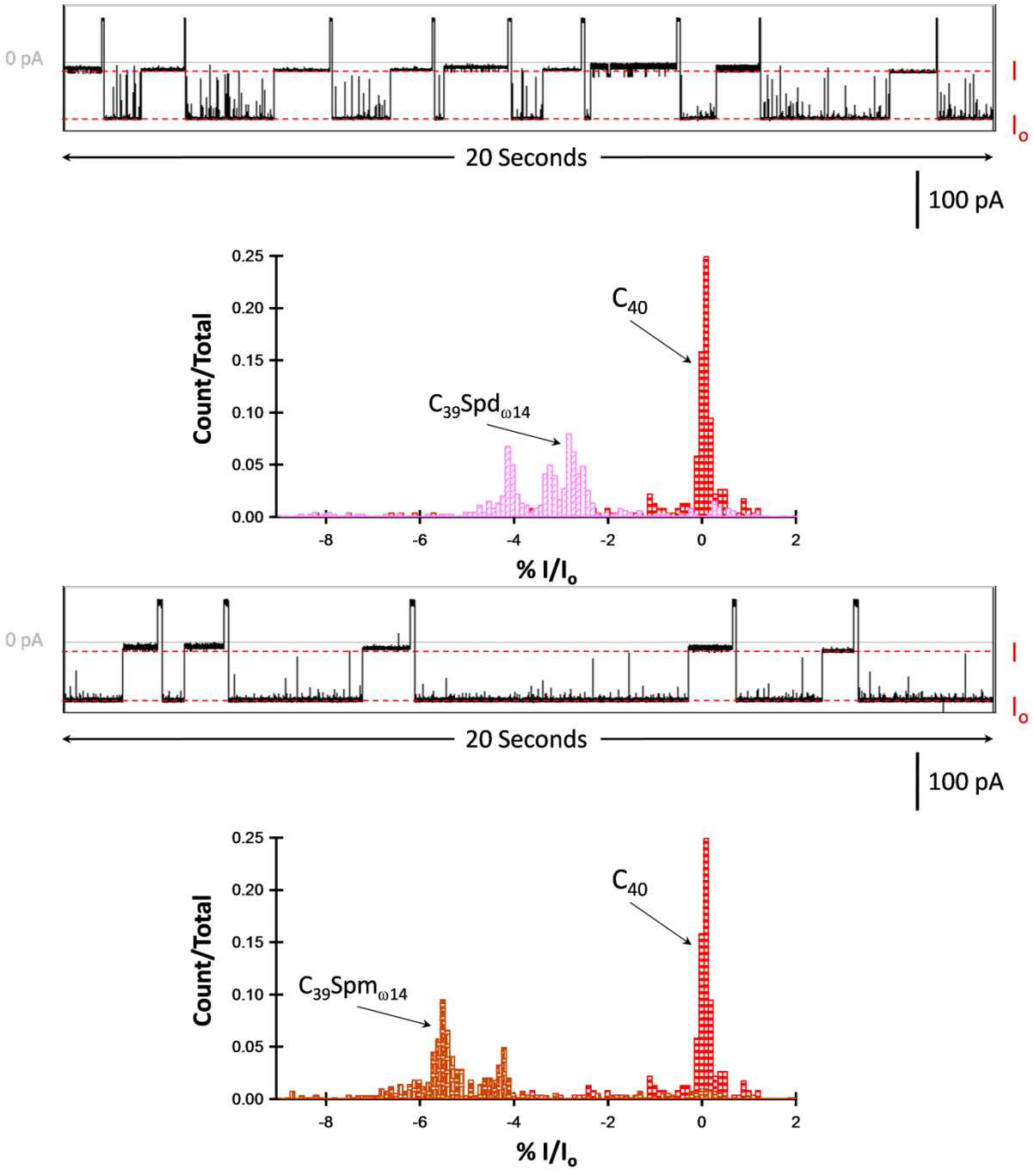

Figure SI 8. Example *i-t* trace for Strep-Btn $C_{39}GPRP_{\omega 14}$ and $\%I/I_o$ histogram compared with Strep-Btn C_{40}. The glycine-proline-arginine-proline amide adduct produced the deepest current blockages events relative to other adducts in this study. There was a large spread in current blockage levels as well as noise amplitude, and a relatively strong peak $\%I/I_o = 0$. The presence of this peak may indicate that the molecule is too large to enter the sensing region of the αHL channel and the surrounding poly-dC sequence is being occasionally detected.

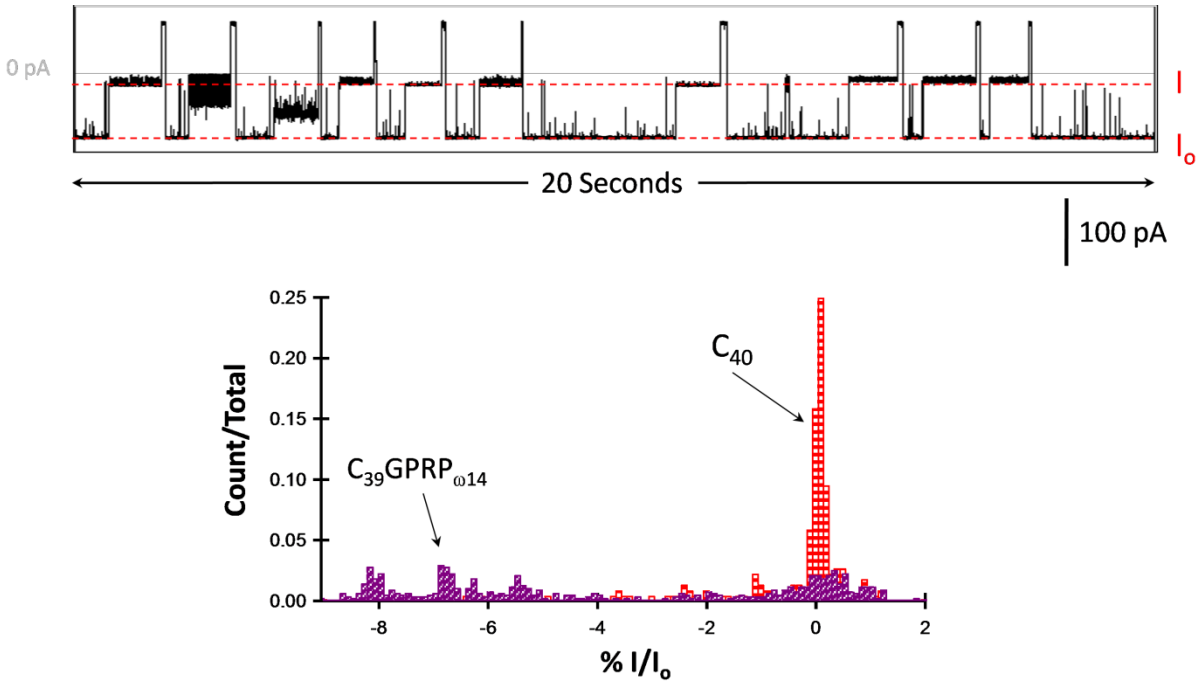

Figure SI 9. Example *i-t* trace for Strep-Btn Kras-$G_{\omega 14}$ and the resulting %I/I_o histogram compared with Strep-Btn C_{40}. Strep-Btn Kras-$G_{\omega 14}$ produces current blockage levels similar to Strep-Btn C_{40}, but with a larger spread.

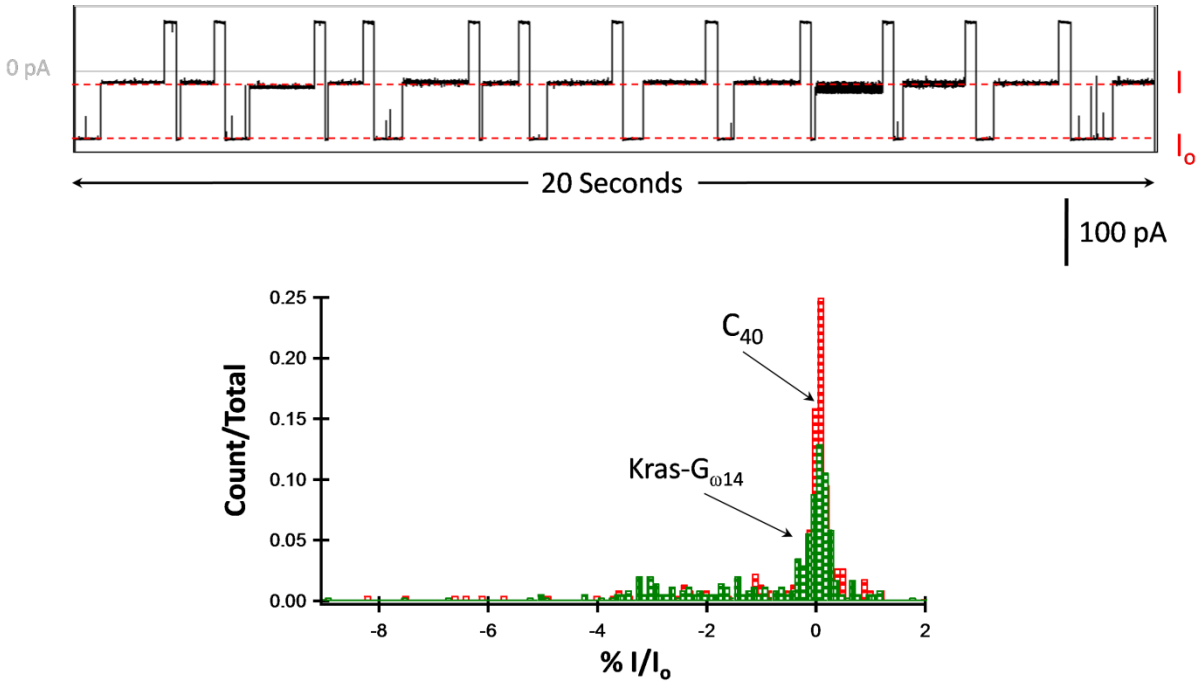

Figure SI 10. Example *i-t* traces for Strep-Btn Kras-$OG_{\omega 14}$ and the resulting %I/I_o histogram compared with Strep-Btn Kras-$G_{\omega 14}$.

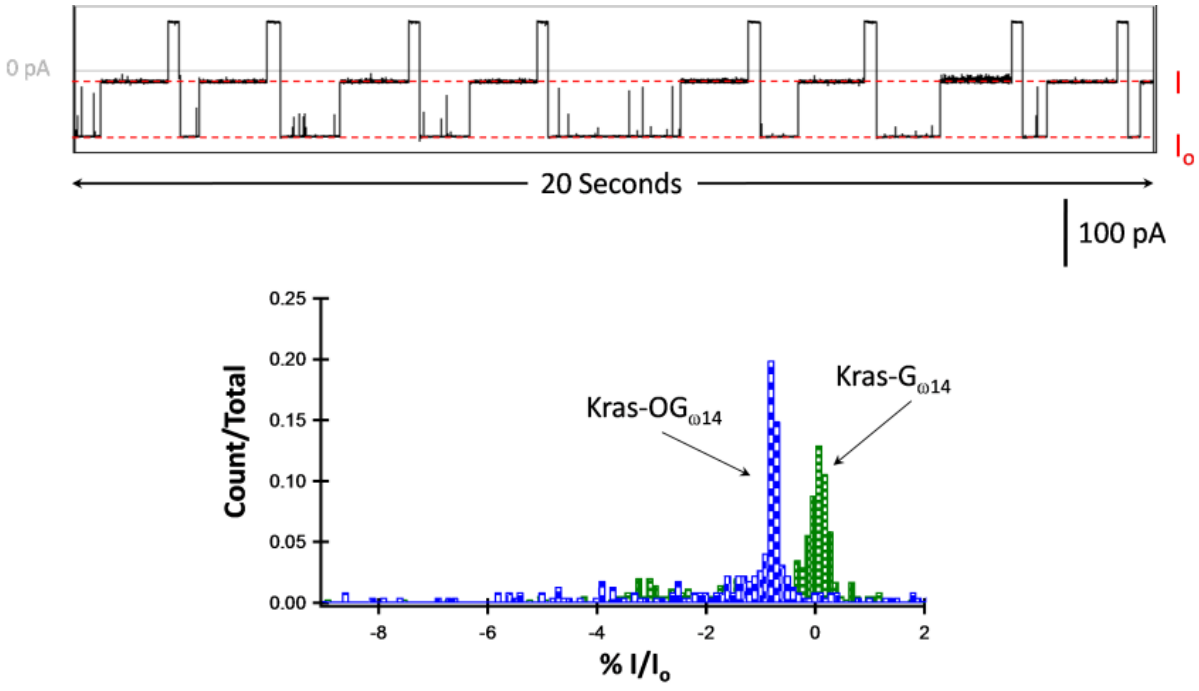

Figure SI 11. Example *i-t* traces for Strep-Btn Kras-Sp$_{\omega 14}$ (upper) and Strep-Btn Kras-Gh$_{\omega 14}$ (lower), and the resulting %I/I$_o$ histograms compared with Strep-Btn Kras-G$_{\omega 14}$.

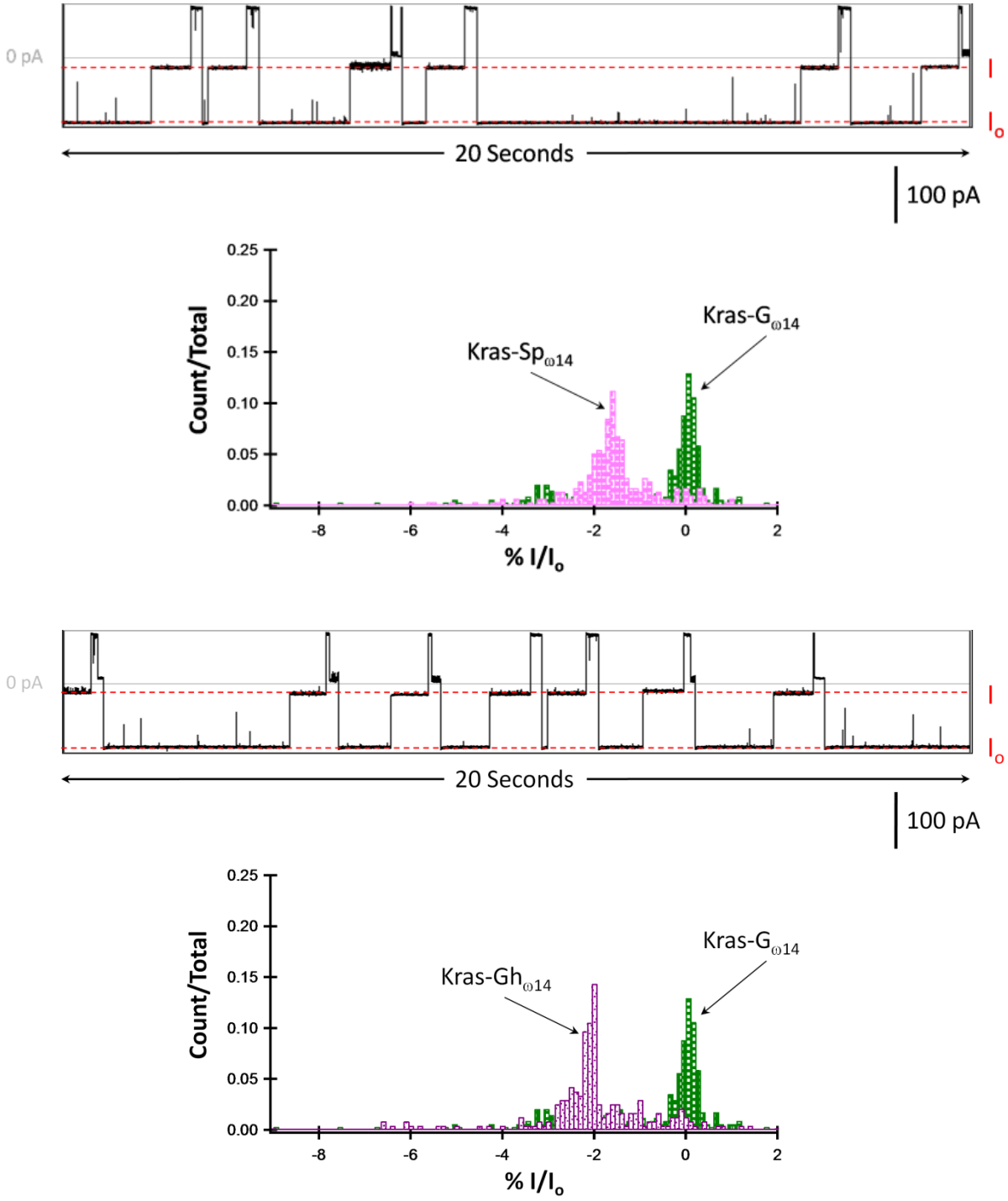

Figure SI 12. Example *i-t* trace for Strep-Btn Kras-Spm$_{\omega 14}$ and %I/I$_o$ histogram compared with Strep-Btn Kras-G$_{\omega 14}$. Strep-Btn Kras-Spm$_{\omega 14}$ yields deeper current blockages relative to Strep-Btn Kras-G$_{\omega 14}$, and a single %I/I$_o$ peak that is sharper relative to Strep-Btn C$_{39}$Spm$_{\omega 14}$.

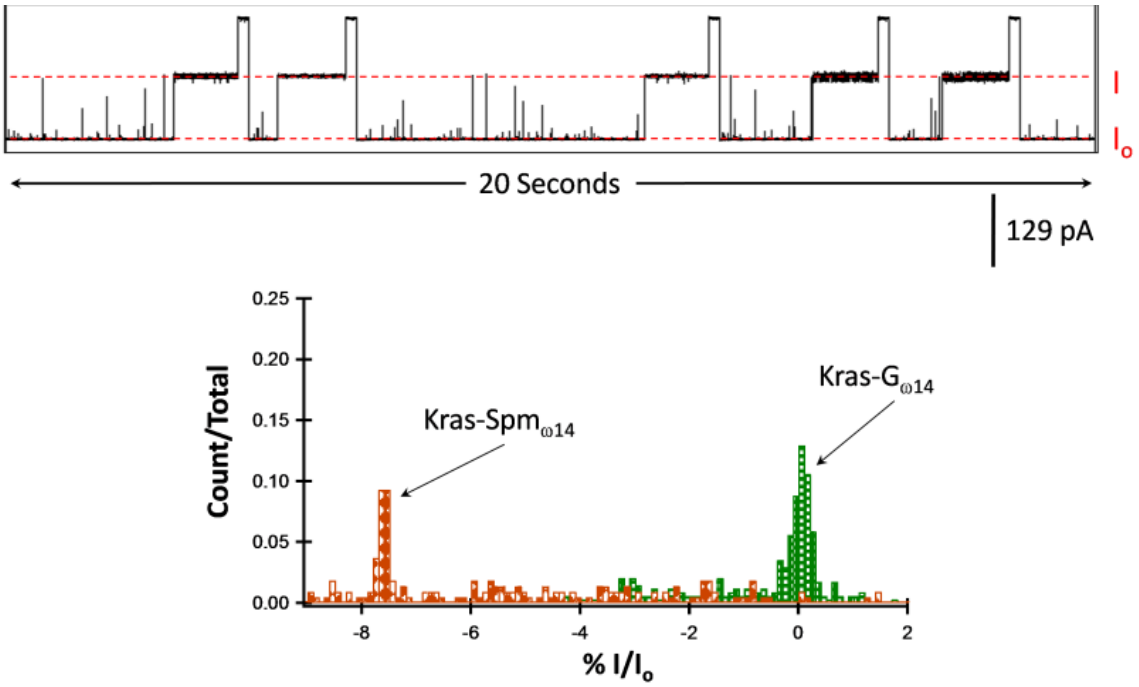

Figure SI 13. $\%I/I_o$ histograms for native base substitutions at position ω14 within a poly-dC background, Strep-Btn $C_{39}X_{\omega 14}$, where X = A, T, or G. Strep-Btn C_{40} is used as a reference sample; the $\%I/I_o$ for Strep-Btn C_{40} is set to 0 and $\%I/I_o$ for all other samples is relative to Strep-Btn C_{40}. Differences in the residual current for native base substitutions at position ω14 in a poly dC background have been previously reported.[7] The relative positions shown here are consistent, but possess smaller absolute residual current differences, this variation in contrast is attributed to differing experimental conditions.

C_{40}-Btn 5'- CCCCCCCCCC CCCCCCCCCC CCCCCC$X_{\omega 14}$CCC CCCCCCCCCC -Btn

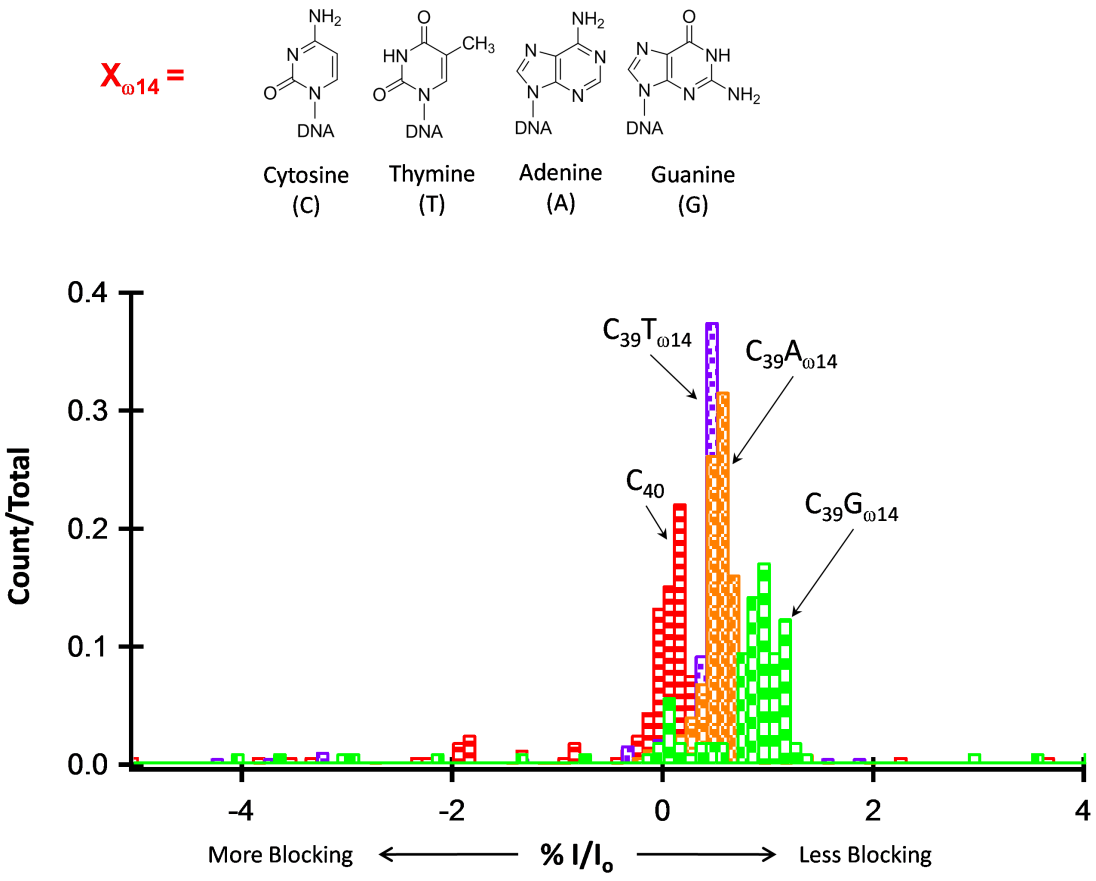

Figure SI 14. Current blockage histograms for Strep-Btn $C_{39}X_{\omega 14}$, where X = C, T, A, G, OG, Sp, and Gh. Strep-Btn C_{40} is used as a reference sample; the $\%I/I_o$ for Strep-Btn C_{40} is set to 0 and $\%I/I_o$ for all other samples is relative to Strep-Btn C_{40}.

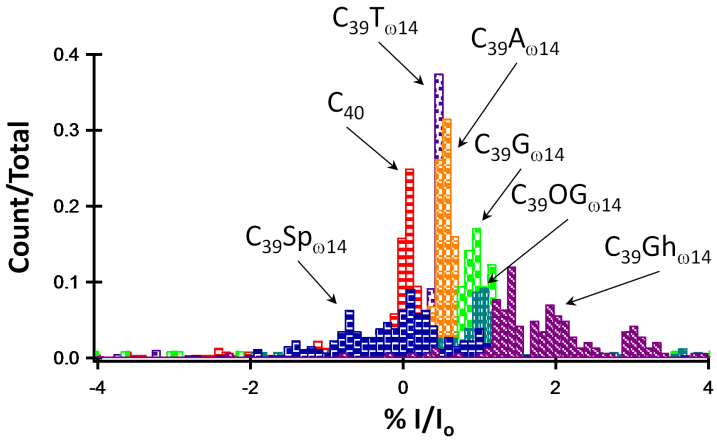

Figure SI 15. Current blockage histograms for Strep-Btn $C_{39}X_{\omega 14}$, where X = C, T, A, G, Lys, Bz, GlcN, Spd, Spm, and GPRP. C_{40} was used as a reference sample; the $\%I/I_o$ for C_{40} was set equal to 0, and $\%I/I_o$ for all other samples is relative to C_{40}.

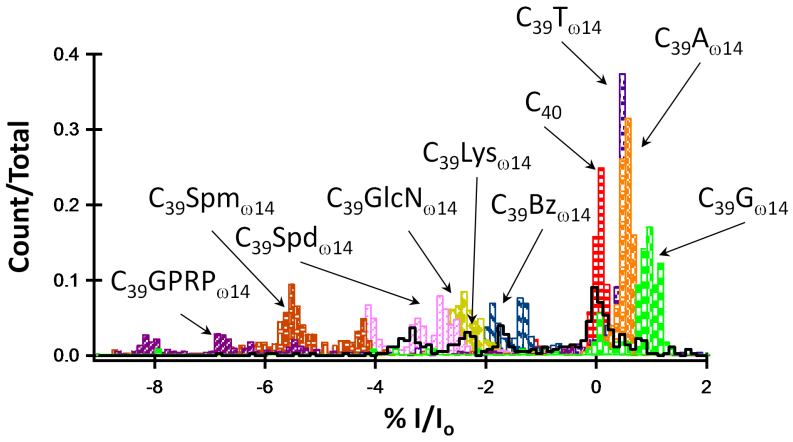

References

(1) Kornyushyna, O.; Berges, A. M.; Muller, J. G.; Burrows, C. J. In vitro nucleotide misinsertion opposite the oxidized guanosine lesions spiroiminodihydantoin and guanidinohydantoin and DNA synthesis past the lesions using Escherichia coli DNA polymerases I (Klenow Fragment). *Biochemistry* **2002,** 41, 15304-15314.

(2) Hosford, M. E.; Muller, J. G.; Burrows, C. J. Spermine participates in oxidative damage of guanosine and 8-oxoguanosine leading to deoxyribosylurea formation. *J. Am. Chem. Soc* **2004,** 126, 9540-9541.

(3) Xu, X.; Muller, J. G.; Ye, Y.; Burrows, C. J. DNA-protein cross-links between guanine and lysine depend on the mechanism of oxidation for formation of C5 vs C8 guanosine adducts. *J. Am. Chem. Soc* **2008,** 130, 703-709.

(4) Zhang, G.; Zhang, Y.; White, H. S. The nanopore electrode. *Anal. Chem.* **2004**, *76*, 6229-6238.

(5) Zhang, B.; Galusha, J.; Shiozawa, P. G.; Wang, G.; Bergren, A. J.; Jones, R. J.; White, R. J.; Ervin, E. N.; Cauley, C. C.; White, H. S. Bench-top method for fabricating glass-sealed nanodisk electrodes, glass nanopore electrodes, and glass nanopore membranes of controlled size. *Anal Chem.* **2007**, *79*, 4778-4787.

(6) White, R. J.; Ervin, E. N.; Yang, T.; Chen, X.; Daniel, S.; Cremer, P. S.; White, H. S. Single ion-channel recordings using glass nanopore membranes. *J. Am. Chem. Soc.* **2007**, *129*, 11766-00775.

(7) Stoddart, D.; Heron, A. J.; Mikhailova, E.; Maglia, G.; Bayley, H. *Proc. Natl. Acad. Sci.* **2009**, *106*, 7702-7707.